Mesoscale physical features and the patchiness of zooplankton and nekton in the northern California Current System

OS31D-59

by P. H. Ressler, R.D. Brodeur, W.T. Peterson, NOAA-NMFS-Northwest Fisheries Science Center, Hatfield Marine Science Center, Newport, OR 97365-5296 (Patrick.Ressler@noaa.gov)
S.D. Pierce, College of Oceanic and Atmospheric Sciences, Oregon State University, Corvallis, OR 97331-5503

Introduction

Zooplankton and nekton populations were surveyed using both nets and acoustics during multidisciplinary GLOBEC (Global Ocean Ecosystems Dynamics) fieldwork in the northern California Current System (CCS) during August 2000. The interaction of seasonal upwelling and mesoscale eddies clearly influenced spatial patterns: chlorophyll concentrations, zooplankton biomass, seabird biomass, and the densities of fish and marine mammals were all elevated in meanders of the California Current off of Heceta Head and Cape Blanco, Oregon, relative to other parts of the study area (Figure 1). To test the hypothesis that aggregations of zooplankton and nekton were larger and more numerous in these apparently productive waters than in other parts of the study area, patch definition methods based on image analysis techniques were applied to multifrequency acoustic backscatter data. This poster shows preliminary results of those analyses.

Chinook and coho salmon, humpback whales, temperature at 5 m | *Copepod biomass, seabird biomass, chlorophyll at 5 m* | *Cruise tracks*

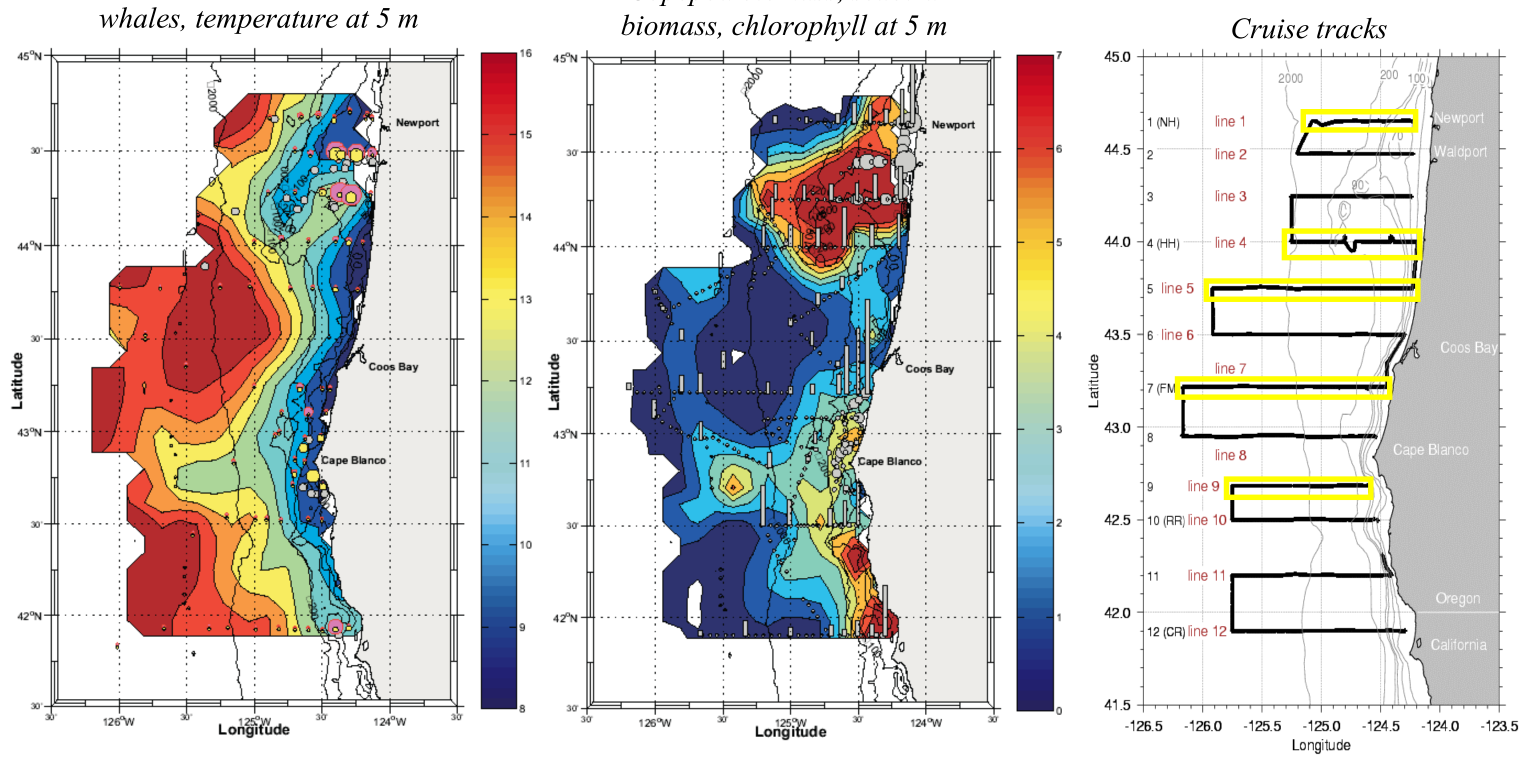

Figure 1.

Left Panel. Color contours show temperature (ºC) at 5 meters depth from sensors on a towed SeaSoar undulator. Yellow and magenta circles are abundances of juvenile chinook and coho salmon, respectively. The largest circles represent catches of ca. 10 fish per standard trawl. The grey circles represent sightings of humpback whales. Note that juvenile salmon were found over the shelf only, and humpback whales were concentrated on Heceta Bank and near Cape Blanco.

Middle Panel. Color contoured chlorophyll concentration (mg m^{-3}) at 5 meters depth, showing highest concentrations over Heceta Bank and nearshore south of Cape Blanco. Gray circles depict bird biomass (kg km^{-2}); largest circles represent 170 kg km^{-2}. Histograms (bars) indicate total copepod biomass (mg m^{-3}) from vertical plankton tows spanning the upper 100m or near bottom (if shallower). Tallest bars represent copepod biomass of 65 mg m^{-3}. Note the concentration of bird biomass nearshore and copepod biomass nearshore and on Heceta Bank.

These panels prepared by Hal Batchelder (see Acknowledgements).

Right Panel. Acoustic survey cruise track, with east-west transects shown on this poster highlighted in yellow (modified from plot located at http://damp.coas.oregonstate.edu/globec/nep/).

Methods: analyzing acoustic backscatter data

From July 30 through August 4, the R/V *Wecoma* made twelve ~ 80 - 130 km east-west transects off of Oregon and northern California, beginning off Crescent City, CA and ending off of Newport, OR. Raw acoustic data collected using a towed four-frequency Hydroacoustics Technology Incorporated (HTI) echosounder were processed using custom software routines written in Visual Basic and Matlab. Data streams included volume backscattering strength at 38, 120, 200, and 420 kHz echointegrated for 12 second intervals, as well as the time, location, and distance from the transducer in 1 m vertical bins for each measurement. The ping rate was once per second at each frequency.

Since the horizontal distance covered by each acoustic sample and the depth of the tow vehicle varied with ship speed, only data collected when the ship was steaming at transit speeds of approximately 8 knots or 14.8 km/hr were analyzed here. At 8 knots, the ship covered about 50 m of horizontal distance and acoustically sampled between approximately 8 m and 204 m in the water column, depending on acoustic frequency. If there were large gaps due to missing data, the transect line was divided into uninterrupted sections for analysis.

Frequency differencing and image analysis

Defining zooplankton and nekton patches relies on the fact that the acoustic backscatter measurement is more sensitive to small targets as frequency increases and wavelength decreases. Scattering models for various anatomical classes of zooplankton (e.g. gas-bearing, elastic-shelled, fluid-like; Stanton et al., 1944) and for fish (e.g., Clay and Horne, 1994) confirm this general frequency-dependent behavior.

This frequency-dependence is the basis for methods which invert acoustical backscatter measurements into estimates of zooplankton concentrations by explicit use of zooplankton scattering models (e.g. Holliday and Pieper, 1995; Pierce et al., 2002), or classify different types of biological targets on the basis of multifrequency acoustic measurements (Horne, 2000). 'Differencing' between frequencies has been used by other authors to differentiate between fish and zooplankton in acoustic survey data (e.g. Madureira et al., 1993; Mitson et al., 1996; Swartzman et al., 1994, 1999). Here, frequency differencing and image processing techniques based on the work of Swartzman et al. were used to identify patches of zooplankton and fish in the echogram images (Figure 2, Table 1).

Figure 2. *Steps in selection of patches from acoustic images*

1. Bottom and false bottom reflections were removed from the original backscatter image.

2. Only pixels greater than a chosen threshold were retained for possible inclusion in a patch (we defined the densest aggregations as the patches of interest.) Thresholds were selected based on the arithmetic mean + 1.5 standard deviations of all the pixels in the images analyzed.

When a pair of frequencies were used to define a patch, backscatter in a given pixel had to both exceed the threshold and be 2 dB greater at the higher frequency to be included.

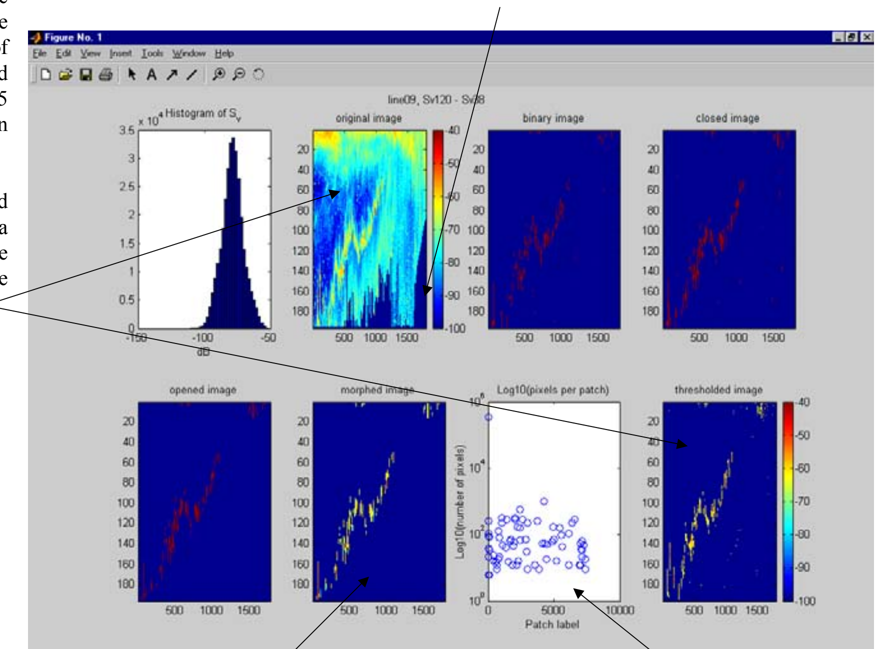

3. Pixels were smoothed into patches using a 'closing' followed by an 'opening' with a 3x3 pixel square structuring element. Then, the members of each defined patch of contiguous pixels were labeled with a connected-component operator. These image processing algorithms are described by Haralick and Shapiro (1992).

4. Calculate patch area based on the number of pixels in a patch and the approximate pixel size.

Acknowledgments: In Figure 1, SeaSoar data are courtesy of Jack Barth and Tim Cowles, whale sighting data are courtesy of Cynthia Tynan, and bird biomass estimates are courtesy of David Ainley. Anders Røstad counted zooplankton from the MOCNESS tows shown in Figure 4, in addition to providing data processing code and advice. Gordie Swartzman provided invaluable discussions of his image analysis and acoustic patch definition methods, which helped me get started. Jack Barth was extremely helpful in retrieving acoustic data from archives at the last minute for my use on this poster. Patrick Ressler was supported by a National Research Council (NRC) Post-Doctoral Associateship. Field data collection was funded by the GLOBEC Northeast Pacific Program (http://globec.oce.orst.edu/groups/nep/).

Results: patch definition and analysis

Figure 3. Data from five transects (those highlighted in Figure 1) are shown. See Table 1 for a key to the patch colors. Some basic patch statistics are shown in Table 2.

Acoustic volume backscattering strength (S_v, dB re 1 m^{-1}) at four frequencies → *Patches defined based on frequency dependence and image analysis*

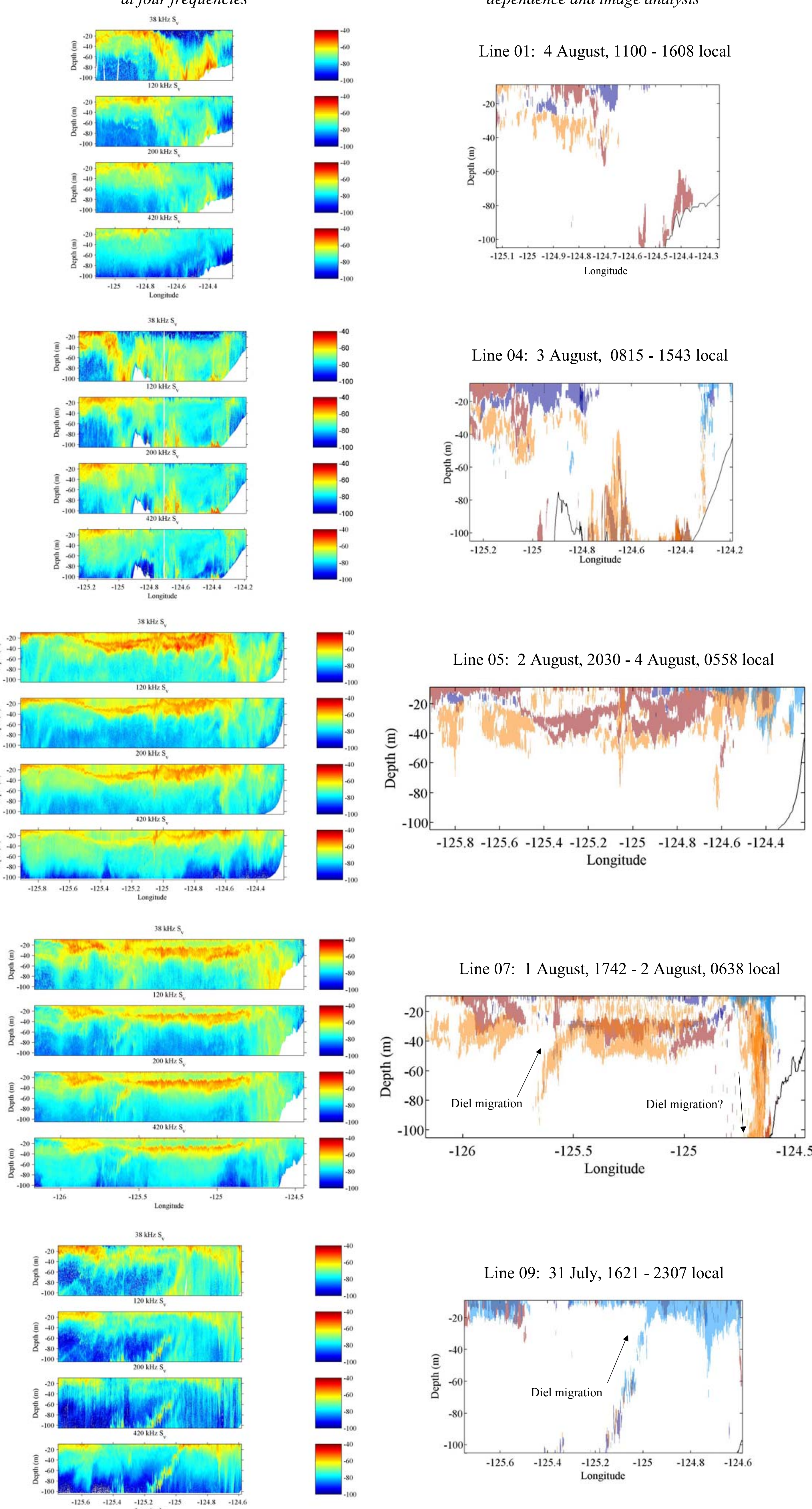

Patches, net tows, individual target strengths

Figure 4. Comparison of average 38 kHz target strength (TS) of individually tracked acoustic targets, patches of "fish" and "large zooplankton and micronekton," and a plot of zooplankton densities from two 1 m^2 MOCNESS tows made concurrently with acoustic data collection. All data were collected on transect line 04; other data from this line are shown in the second row from the top of Figure 3.

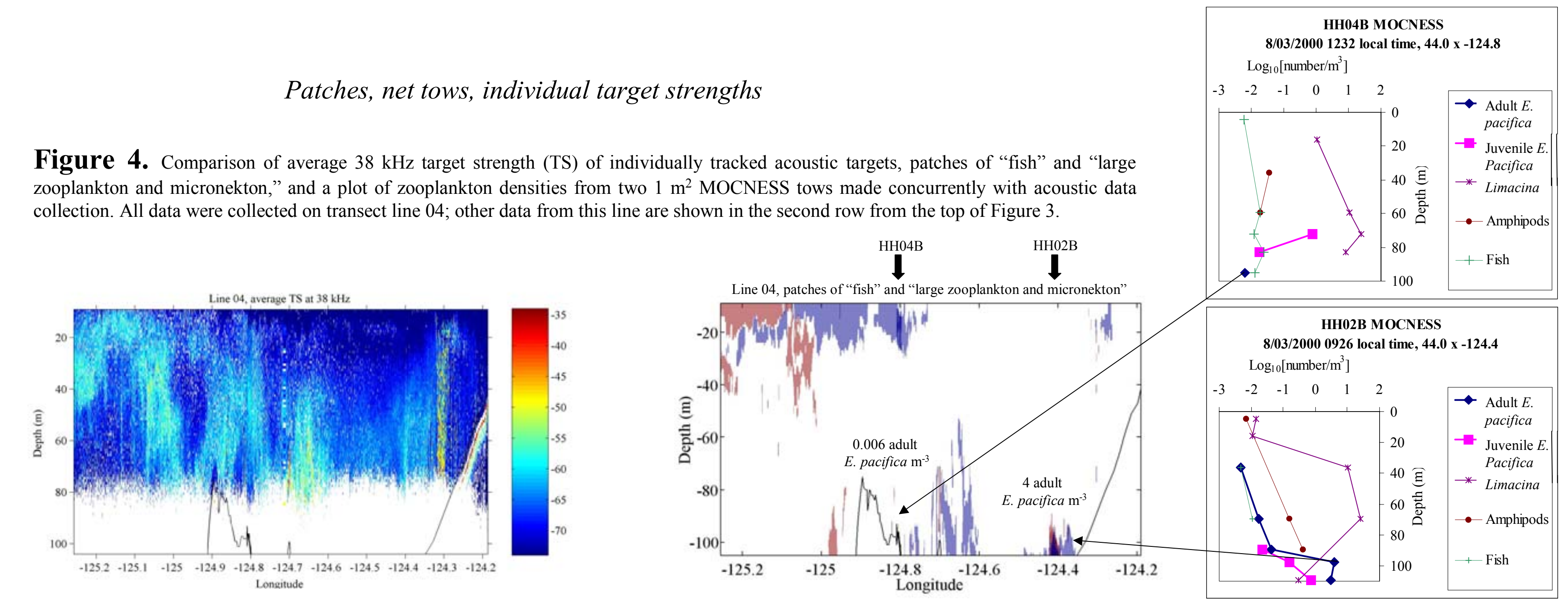

Left panel. Average TS values at 38 kHz suggest that in shallower bins, "fish" targets may have been smaller fish (TS on the order of -55 dB, rather than order -35 dB). In deeper bins, however, it appears that larger fish with higher TS were detected. When strong targets appeared only in isolated pixels, they were not picked up by the patch algorithm. *Note:* TS averages were computed by converting TS in a pixel to linear units, finding the mean, and then converting back to dB.

Right panel. Where the analysis suggests an aggregation of large zooplankton (MOCNESS HH02B), adult *E. pacifica* numbered ~ 4 m^{-3}. In contrast, where no patches of large zooplankton were defined acoustically, MOCNESS HH04B caught < 0.006 adult *E. Pacifica* per m^3. The relatively large number of *Limacina* pteropods do not appear to have caused strong scattering at 38 or 120 kHz (although they may have been detected as "small zooplankton," light blue in the second panel from the top of Figure 3).

Patch definition

Table 1

	Category	Potential constituents	Volume backscatter variables used to define patch	Approximate wavelength of acoustic frequencies used (mm, assuming speed of sound in seawater is 1500 m/s)	S_v threshold for inclusion in patch (dB)
(red)	**"Fish"**	fish with gas-filled swimbladders	S_{v38}	39	-58
(dark blue)	**"Large Zooplankton and Micronekton"**	adult euphausiids, small fish without gas-filled swimbladders	S_{v120} - S_{v38}	13, 39	-66
(orange)	**"Medium Zooplankton"**	smaller euphausiids, amphipods	S_{v200} - S_{v120}	8, 13	-68
(light blue)	**"Small Zooplankton"**	large copepods, juvenile euphausiids, pteropods	S_{v420} - S_{v200}	4, 8	-68

Patch number and area

Table 2

Transect	Category	Median cross-sectional area of patches (m^2)	N	Number of patches per distance along transect (#/km)
Line 01	Fish:	1600	23	0.31
	Large Zooplankton:	1250	25	0.34
	Medium Zooplankton:	1350	46	0.62
	Small Zooplankton:	400	1	0.01
Line 04 (mean of two sections)	Fish:	2525	12	0.23
	Large Zooplankton:	4550	18	0.33
	Medium Zooplankton:	1150	35	0.64
	Small Zooplankton:	888	11	0.21
Line 05	Fish:	1200	41	0.30
	Large Zooplankton:	1425	44	0.32
	Medium Zooplankton:	1100	124	0.91
	Small Zooplankton:	1000	53	0.39
Line 07 (longest section only)	Fish:	900	65	0.55
	Large Zooplankton:	1050	67	0.57
	Medium Zooplankton:	1000	171	1.44
	Small Zooplankton:	450	51	0.43
Line 09	Fish:	1350	33	0.35
	Large Zooplankton:	1050	35	0.37
	Medium Zooplankton:	1050	36	0.38
	Small Zooplankton:	1775	56	0.59

Preliminary conclusions

- This method serves as an interpretive tool, extracting ecologically meaningful information from multifrequency acoustic data. It complements other approaches to analysis of such datasets (see Pierce et al., 2002, this session).
- Identified patches of "large zooplankton and micronekton" compared well with adult euphausiid densities from two MOCNESS tows.
- "Fish" patches did not compare well with catches from 30 m x 20 m Nordic rope trawls taken at the surface (not shown). Likewise, although "fish" patches identified in deeper bins compared fairly well with average 38 kHz TS distributions, "fish" patches at the surface did not. This may reflect differences in selectivity and sampling volume of the acoustic beam in the upper depth bins (m^3 - 10^2 m^3) versus the trawl (10^6 m^3). Adjustments to processing parameters and fuller utilization of target strength data may lead to improvements.
- Lines 1 and 4 contained the largest patches (by area) of large and medium zooplankton. In contrast, Line 07 had the smallest patches in these categories and 1.5 - 2 times more patches per km of transect. These preliminary findings may reflect changes in zooplankton distribution due to mesoscale physical forcing, which could produce persistent enhancement of epipelagic nutrients, retention of plankton, and/or elevated primary and secondary production.
- Other useful statistics can be calculated on patches identified by this method (e.g. Nero and Magnuson, 1989; Swartzman et al. 1999), which may complement spatial series analysis to determine characteristic scales of variability in plankton and nekton stocks.
- Analysis of patch size and distribution may be useful in understanding the influence of spatial variability in plankton and fish distribution on the foraging potential of different habitats for higher predators, such as salmon, seabirds, and marine mammals.

References:

Clay, C.S. and Horne, J.K., 1994. Acoustic models of fish: The Atlantic cod (*Gadus morhua*). Journal of the Acoustical Society of America 96(3), 1661- 1668.
Haralick, R.M. and Shapiro, L.J., 1992. Computer and robot vision, Volume 1. Addison-Wesley, Reading, MA, 672p.
Holliday, D.V., Pieper, R.E., 1995. Bioacoustical oceanography at high frequencies. ICES Journal of Marine Science 52(3/4), 297-304.
Horne, J.K., 2000. Acoustic approaches to remote species identification. Fisheries Oceanography 9(4), 356-371.
Nero, R.W. and Magnuson, R.W. 1989. Characterization of patches along transects using high-resolution 70-kHz integrated acoustic data. Canadian Journal of Fisheries and Aquatic Sciences 46, 2056-2064.
Mitson, R.B., Simard, Y., Goss, C., 1996. Use of a two-frequency algorithm to determine size and abundance of plankton in three widely spaced locations. ICES Journal of Marine Science 53(4), 209-215.
Madureira, L.S.P., Everson, I., Murphy, E.J., 1993. Interpretation of acoustic data at two frequencies to discriminate between Antarctic krill (*Euphausia superba* Dana) and other scatterers. Journal of Plankton Research 15(7), 787-802.
Pierce, S. D., Barth, J.A., Peterson, W. T., Cowles, T. J., 2002. Bio-acoustic Surveys in the Northern California Current System. Ocean Sciences poster OS31D-58.
Stanton, T.K., Wiebe, P.H., Chu, D., Benfield, M.C., Scanlon, L., Martin, L., Eastwood, R.L., 1994. On acoustic estimates of zooplankton biomass. ICES Journal of Marine Science 51, 505-512.
Swartzman, G., Stuetzle, W., Kulman, K., Wen, N., 1994. Modeling the distribution of fish schools in the Bering Sea: Morphological school identification. Natural Resource Modeling 8(2), 177-194.
Swartzman, G., Brodeur, R., Napp, J., Walsh, D., Hewitt, R., Demer, D., Hunt, G., Logerwell, E., 1999. Relating spatial distributions of acoustically determined patches of fish and plankton: data viewing, image analysis, and spatial proximity. Canadian Journal of Fisheries and Aquatic Sciences 56, 188-198.